Formation of cold molecular filaments in cooling flow clusters

Yves Revaz[1], Françoise Combes[1] & Philippe Salomé[2]

[1]LERMA, Observatoire de Paris, 61 av. de l'Observatoire, 75014 Paris, France, [2]IRAM, 300 rue de la piscine, 38400 St-Martin d'Hères, France

New CO observations at the center of cooling flow in Perseus cluster (Salomé et al. 2006) show a clear correlation of the molecular gas with the previously detected H-α filaments (Conselice et al. 2001). In this poster, we present high resolution multi-phase simulations of the Perseus Cluster, taking into account the AGN feedback in form of hot buoyant bubbles. These simulations show that significant amount of gas can cool in cooling flow clusters, in spite of the AGN feedback. The latter provides some heating, but also trigger the hot gas compression, that favours cooling, even at high radius ($R > 30\,\mathrm{kpc}$). The time spent by the gas in the intermediate temperature phase ($10^7\,\mathrm{K}$ to $10^4\,\mathrm{K}$) is so short, that no gas is expected to be observed below 1 KeV in X-rays. The cooled gas flows into the cluster core forming the observed filaments.

Initial Conditions

Our cluster model is designed to fit the Perseus X-ray data of Sanders et al. (2003). The total mass distribution profile follows a pseudo-isothermal sphere :

$$\rho(r) = \frac{\rho_0}{1+\left(\frac{r}{r_c}\right)^2}, \qquad (1)$$

with $\rho_0 = 1.4 \times 10^7\,\mathrm{M_\odot kpc^{-3}}$ and $r_c = 40\,\mathrm{kpc}$. The mass distribution is truncated at $R = 2\,\mathrm{Mpc}$ and the total mass is $5.5 \times 10^{14}\mathrm{M_\odot}$. The gas corresponding to 15% of the total mass has an initial temperature of $2.8 \times 10^7\,\mathrm{K}$.

Multiphase intra-cluster gas

The bulk of the intra-cluster gas has at high temperature ($10^7\,\mathrm{K}$) is well modeled by an ideal gas with adiabatic index of 5/3. This hot phase has been computed using and SPH technique. For lower temperatures, SPH is not suited to render the clumpiness of the gas. Below $10^4\,\mathrm{K}$, the gas is treated as semi-collisional, using a sticky particle technique (Combes & Gerin, 1985). Star formation may occur in this cold phase, following a Schmidt law. The cooling of the hot gas is computed using the data of Sutherland & Dopita (1993), assuming an abundance of one third of the solar one.

AGN feedback

Following Sijacki & Springel (2006) the AGN feedback is modeled by injecting energy in hot intra-cluster gas bubbles which are then driven buoyantly at higher radius. Bubbles are defined by their position R, diameter D, temperature T_b, over pressure p and angle α (angle of the bubble with respect to the y axis). They are generated by symmetric pairs, in average each 200 Myr. Bubbles parameters are randomly chosen in the ranges given by Tab. 1. and are actually not correlated to the cluster accretion rate.

Radius R	$50-60\,\mathrm{kpc}$
Diameter D	$20-40\,\mathrm{kpc}$
Over pressure p	$1-2$
Temperature T_b	$5\times10^7-2\times10^8\,\mathrm{K}$
Angle α	$0-360$

Tab. 1. Interval parameters for the bubbles.

The specific energy (u_b) and density (ρ_b) of particles in a bubble are given by :

$$u_b = \frac{1}{\gamma-1}\frac{k_B T_b}{\mu m_H} \quad \text{and} \quad \rho_b = p\rho_i\frac{u_i}{u_b} \qquad (2)$$

where ρ_i and u_i corresponds to the unperturbed intra-cluster gas density and specific energy at the same radius.

Numerical technique

The simulations have been run using a modified version of the Gadget2 Tree-SPH code (Springel, 2005), including cooling, star formation and multiphase SPH/Sticky gas. In each simulations the gas is represented by 4'194'304 SPH particles. The dark matter is modeled by a fixed outer potential.

Evolution of an isolated bubble

Fig. 1. show the evolution of an isolated bubble. The bubble is generated at $t = 0$ ($R = 50\,\mathrm{kpc}$, $D = 30\,\mathrm{kpc}$, $T = 10^8\,\mathrm{K}$, $p = 2$). At $t = 300\,\mathrm{Myr}$ the bubble is still moving upwards (red in the radial velocity map). It reaches $R = 130\,\mathrm{kpc}$ and takes the characteristic mushroom shape as observed in H-α and X-ray (Fabian et al. 2003). A substantial amount of cooler gas (about 1/2 of the bubble mass) is dragged by the rising bubble and forms the trunk of the mushroom. Between $t = 300-500\,\mathrm{Myr}$, this gas of lower entropy fall back into the cluster center (blue in the radial velocity map), while the head of the mushroom stops and dissipate slowly into the intra-cluster medium.

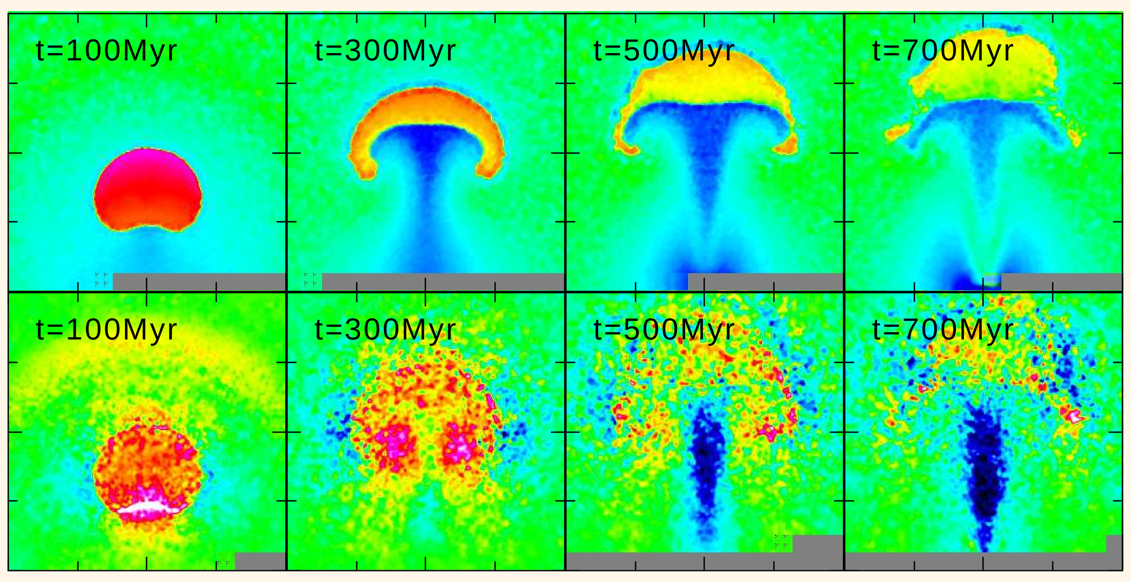

Fig. 1. Evolution of an isolated bubble. Top panels : Temperature from $10^4\,\mathrm{K}$ (black) to $2\times10^8\,\mathrm{K}$ (white). Bottom panels : Radial velocities from $-100\,\mathrm{km/s}$ (black) to $100\,\mathrm{km/s}$ (white) (the model is rotated from 10 degrees around the x axis). The box dimension is $200\times200\,\mathrm{kpc}$.

Global evolution

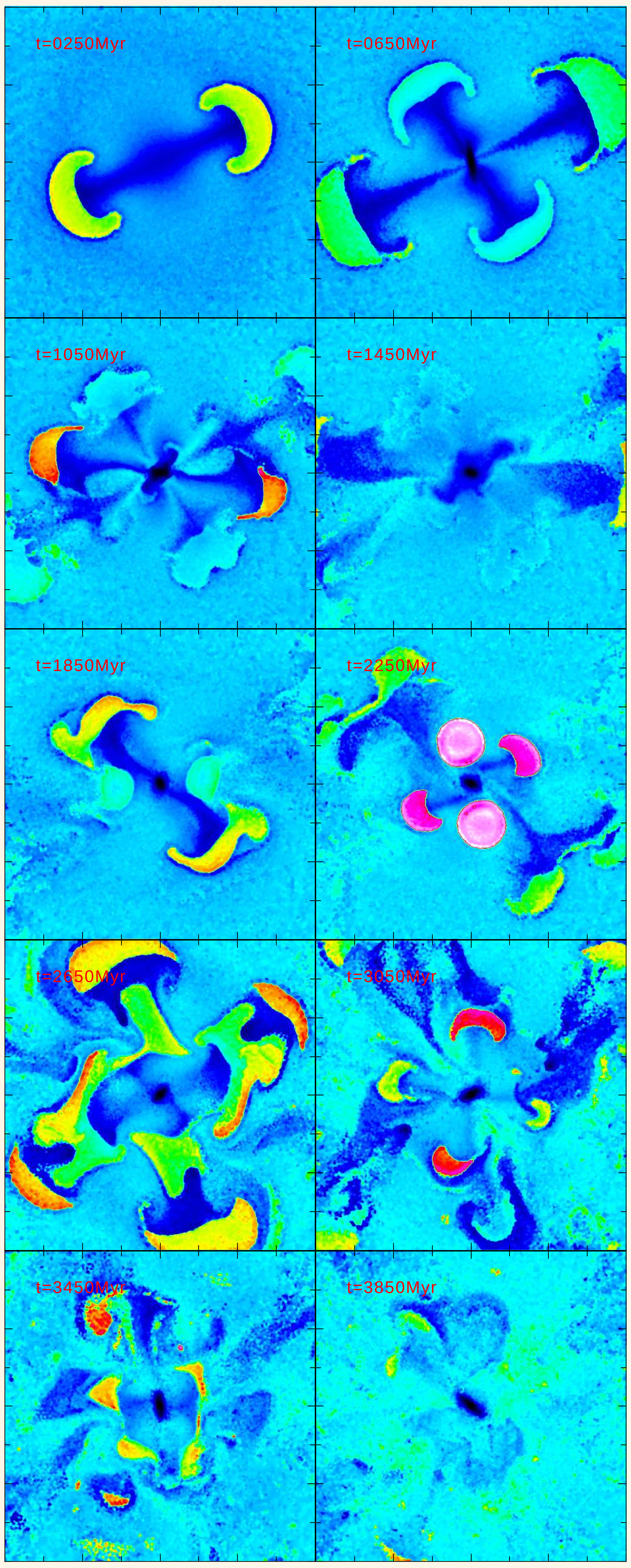

Fig. 2. Evolution of the cluster temperature during 4 Gyr, from $10^4\,\mathrm{K}$ (black) to $2\times10^8\,\mathrm{K}$ (red). The box dimension is $400\times400\,\mathrm{kpc}$.

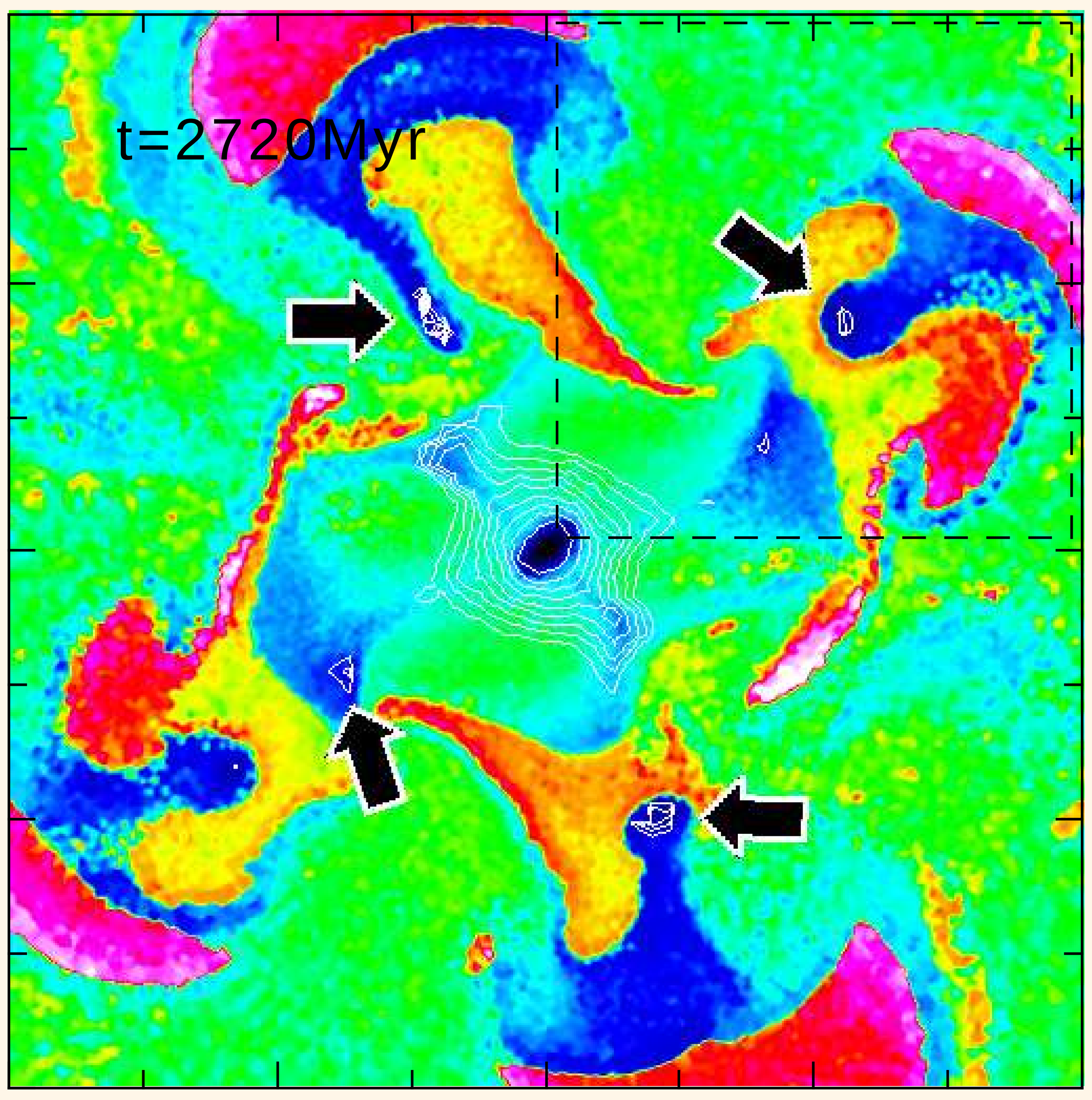

Fig. 3. Gas temperature at $t = 2720\,\mathrm{Myr}$. The white contours (pointed by black arrows) indicate the position of the gas having a short cooling time $\tau_c < 1.1\,\mathrm{Gyr}$ that will be transformed into cold gas in Fig. 4. The upper left box corresponds to the region zoomed in Fig. 4. The box dimension is $400\times400\,\mathrm{kpc}$.

Cold gas formation

In addition to slowing down the cooling flow at the center of the cluster, our simulation also show how AGN feedback may trigger cold gas formation at high radius ($R > 30\,\mathrm{kpc}$). Physical conditions for efficiently cool intra-cluster gas occurs either when the gas is less than $10^7\,\mathrm{K}$ or when its density is sufficiently high. Buoyant bubbles are responsible of strong inhomogeneities in temperature (see Fig. 2) as well as in density of the intra-cluster medium. In Fig. 3, we show how cooler falling gas (trunk of a bubble, see Fig. 1) is trapped between an old and a new rising bubble and is compressed to reach a state where its cooling time is sufficiently short to let the gas becomes cool in a fraction of Gyr. In Fig. 4 the cluster is seen 300 Myr later. The short cooling time gas of Fig. 3 has now cooled down below $10^4\,\mathrm{K}$. As it is not supported by the hot gas pressure, it falls radially to the center, forming a filament like structure ($R = 50$ to $R = 100\,\mathrm{kpc}$) of mass $1.5\times10^8\mathrm{M_\odot}$. In the filament, the gas density is not high enough to form stars.

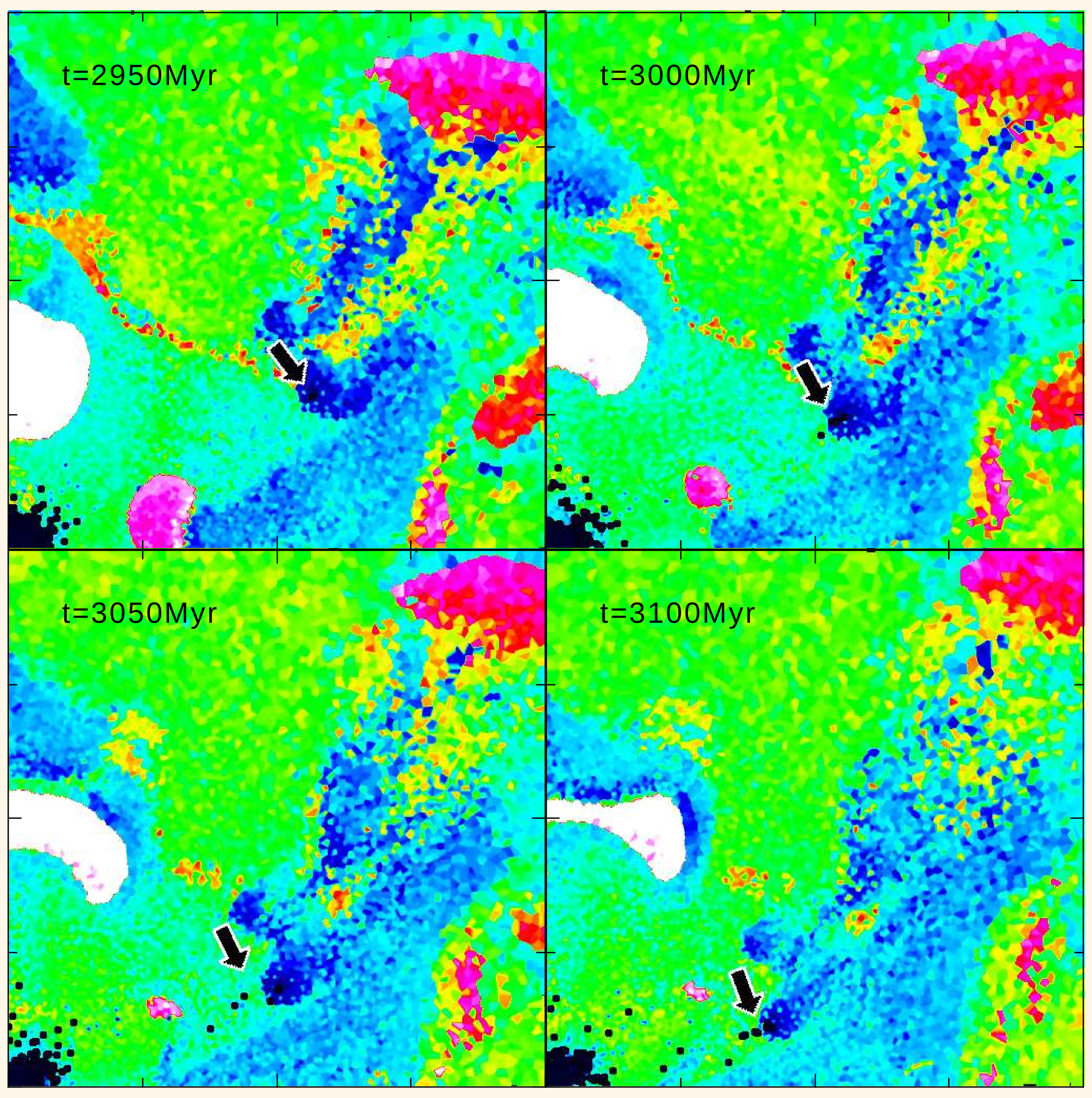

Fig. 4. Gas temperature between $t = 2950\,\mathrm{Myr}$ and $t = 3100\,\mathrm{Myr}$, from $10^4\,\mathrm{K}$ (black) to $2\times10^8\,\mathrm{K}$ (white). The small black dots pointed by the black arrow represents cold gas ($T < 10^4\,\mathrm{K}$ falling into the cluster center. The box dimension of each panel is $200\times200\,\mathrm{kpc}$.)

The lack of emission below 1 KeV

In order to illustrate the very efficient cooling of the gas in over-density regions, Fig. 5. (left) shows the temperature evolution of the gas within the filament of Fig. 4. At $t = 2700$, the gas has a temperature of about $7\times10^6\,\mathrm{K}$. When the temperature of $3\times10^5\,\mathrm{K}$ is reached, the cooling is highly enhanced, causing the gas temperature to quickly fall below $10^4\,\mathrm{K}$. The very short cooling time below $7\times10^6\,\mathrm{K}$ may also explain the paucity of flux detected below 1 keV in cooling flow cluster. The right part of Fig. 5. show an histogram of the mass fraction of gas as a function of its temperature for the whole cluster. It clearly appears that due to its very short cooling time, the gas is very quickly transported from $10^7\,\mathrm{K}$ to $10^4\,\mathrm{K}$, inducing a gap between these two values.

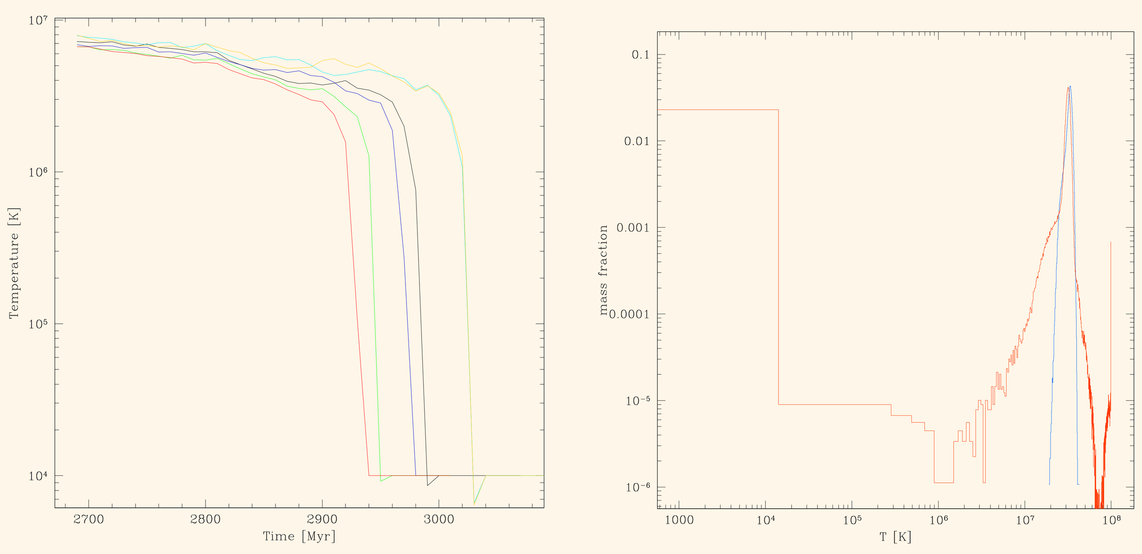

Fig. 5. (a) Temperature evolution of particles within the filament of Fig. 4. (b) Histogram of the mass fraction of gas as a function of its temperature. In blue, at $T = 0$, in red, after 1 Gyr.

References

[2001] Conselice C.J., Gallagher J.S., Wyse R.F.G., 2001, ApJ, 122, 2281

[1985] Combes F., Gerin M., 1985, A&A, 150, 327

[2003] Fabian A.C., Sanders J.S., Crawford C.S., Conselice C.J., Gallagher J.S., Wyse R.F.G., 2003, MNRAS, 344L, 48

[2006] Salomé P., Combes F., Edge A.C., Crawford C., Erlund M., Fabian A.C., Hatch N.A., Johnstone R.M.,Sanders J.S., Wilman R., 2006, in press

[2004] Sanders J.S., Fabian A.C., Allen S.W., Schmidt R.W., 2004, MNRAS, 349, 952

[2006] Sijacki D., Springel V., 2006, MNRAS, 366, 397

[2005] Springel V., 2005, MNRAS, 364, 1105

[1993] Sutherland R.S., Dopita M.A., 1993, ApJS, 88, 253